# Inverse Surface Melting in Confined Clusters: $Ar_{13}$ in Zeolite L†

**R. Chitra‡ and S. Yashonath*,‡,§**

*Solid State and Structural Chemistry Unit and Supercomputer Education and Research Centre, Indian Institute of Science, Bangalore 560012, India*

*Received: June 24, 1996; In Final Form: October 14, 1996*⊗

Monte Carlo and molecular dynamics simulations on an $Ar_{13}$ cluster in zeolite L have been carried out at a series of temperatures to understand the rigid−nonrigid transition corresponding to the solid−liquid transition exhibited by the free $Ar_{13}$ cluster. The icosahedral geometry of the free cluster is no longer preferred when the cluster is confined in the zeolite. The root-mean-squared pair distance fluctuation, $\delta$, exhibits a sharp, well-defined rigid−nonrigid transition at 17 K as compared to 27 K for the free cluster. Multiple peaks in the distribution of short-time averages of the guest−host interaction energy indicate coexistence of two phases. It is shown that this transition is associated with the inner atoms becoming mobile at 17 K even while the outer layer atoms, which are in close proximity to the zeolitic wall, continue to be comparatively immobile. This may be contrasted with the melting of large free clusters of 40 or more atoms which exhibit surface melting. Guest−host interactions seem to play a predominant role in determining the properties of confined clusters. We demonstrate that the volume of the cluster increases rather sharply at 17 and 27 K respectively for the confined and the free cluster. Power spectra suggest that the motion of the inner atoms is generally parallel to the atoms which form the cage wall.

## 1. Introduction

Clusters are widely prevalent in nature.[1] It is necessary to understand their properties as well as the factors determining these properties both for fundamental reasons and because of their industrial importance. Such investigations are expected to provide, in the long run, significant insights into the transition from the finite to bulk behavior and some of the peculiar properties specific to clusters such as the existence of magic numbers. From an application point of view also, such studies would, in all likelihood, provide ways and means of designing tailor-made clusters for use in catalysis, nucleation, etc.

Over the past two decades considerable effort has gone into understanding properties of free clusters.[2−22] Their properties have been studied in great detail, and many good reviews exist on this topic.[23−25] However, clusters are not always found in their free form. They are often found to be enclosed in some host matrix—an inorganic or organic porous solid—or simply attached to a substrate. It is to be expected that the properties of such confined clusters would be different from those of the free clusters. In what way would it be different? Our aim here is to investigate a specific cluster, viz. $Ar_{13}$—a cluster that has been studied thoroughly in its free form—confined in zeolite L. Even though the properties presented in this work pertain specifically to $Ar_{13}$ in the cages of zeolite L, our long-term aim is to derive from such studies general principles governing the behavior of confined clusters.

## 2. Model and Intermolecular Potential

Zeolite L has a structure consisting of channels along the *c* direction. The channels are built up of cagelike units which are interconnected via 12-membered rings. The 12-ring is somewhat elliptical in shape with maximum and minimum diameters of 7.8 and 7.1 Å. The rings are separated by 7.5 Å along the *c* direction. The diameter of the channel is largest (∼13 Å) midway between the two 12-rings. The structure of zeolite L was taken from recent high-resolution neutron powder diffraction studies of Wright et al.[26] Following earlier work, we have chosen to use a highly siliceous zeolite.[27] Zeolite L crystallizes in the *P*6/*mmm* space group with $a = 18.6673$ Å and $c = 7.4956$ Å. One unit cell has a formula $Si_{36}O_{72}$.

Argon atoms interacted via a simple (6−12) Lennard-Jones potential

$$\phi(r_{ij}) = 4\epsilon\left[\left(\frac{\sigma}{r_{ij}}\right)^{12} - \left(\frac{\sigma}{r_{ij}}\right)^{6}\right] \tag{1}$$

The values of $\epsilon$ and $\sigma$ for the Ar−Ar interaction have been taken from the work of Davis et al.[19] The total guest−guest potential energy is therefore given by

$$U_{gg} = \frac{1}{2}\sum_{i=1}^{N}\sum_{j=1,j\neq i}^{N}\phi(r_{ij}) = \frac{1}{2}\sum_{i=1}^{N}u_{gg}(r_i) \tag{2}$$

The cluster atoms interact only with the oxygen atoms of the zeolite framework. The Si atoms of the zeolite are rendered inaccessible due to the presence of the bulkier oxygen atoms. The Ar−O interaction was also modeled in terms of a (6−12) Lennard−Jones form

$$\phi(r_{iz}) = 4\epsilon_{iz}\left[\left(\frac{\sigma_{iz}}{r_{iz}}\right)^{12} - \left(\frac{\sigma_{iz}}{r_{iz}}\right)^{6}\right] \tag{3}$$

where *i* is a cluster atom and *z* is an oxygen atom of the zeolite framework. The self-interaction parameters for the O−O interaction were calculated from the work of Henson et al.[27] The parameters for the Ar−O interaction were then calculated using the well-known Lorentz−Berthelot combination rules.[28] The total guest−zeolite potential energy is given by

$$U_{gh} = \sum_{i=1}^{N}\sum_{z=O}\phi(r_{iz}) = \sum_{i=1}^{N}u_{gh}(r_i) \tag{4}$$

† Contribution No. 1185 from the Solid State and Structural Chemistry Unit.
‡ Solid State and Structural Chemistry Unit.
§ Supercomputer Education and Research Centre.
⊗ Abstract published in *Advance ACS Abstracts,* December 1, 1996.

S1089-5647(96)01872-X CCC: $14.00 © 1997 American Chemical Society

**TABLE 1: Potential Parameters for Guest−Guest and Guest−Zeolite Interactions**

| type | $\sigma$ (Å) | $\epsilon$ (kJ/mol) |
|---|---|---|
| Ar−Ar | 3.4 | 1.005 68 |
| Ar−O | 2.96785 | 1.224 69 |

The total potential energy of the system is the sum of the contributions from the guest−guest and guest−zeolite interactions.

$$U = U_{gg} + U_{gh} \tag{5}$$

The potential parameters for all interactions are listed in Table 1.

## 3. Computational Methods

Simulations have been carried out using Monte Carlo as well as molecular dynamics methods.

The simulation cell consisted of two units cells along each of the *a* and *b* directions and three unit cells along the *c* direction. The zeolite framework was assumed to be rigid. The zeolite merely imposed an external field on the argon cluster. Only the argon atoms were included in the integration.

The Metropolis algorithm was used to perform the Monte Carlo simulations. Every Monte Carlo step consisted of an attempt to move each of the cluster atoms exactly once. Any move that led to an atom being displaced by more than $4\sigma$ from the cluster center of mass (com) was rejected outright.

A spherical cutoff of 10 Å was employed in the calculation of both guest−guest and guest−zeolite interactions. Periodic boundary conditions were imposed.

Every run consisted of an equilibration phase of $10^6$ MC steps, followed by a production run of $7 \times 10^6$ MC steps. Positions and energies were stored every 100 steps which were later used for the calculation of various properties. Short-time averages of the potential energies were calculated over every successive 3500 configurations.

Molecular dynamics calculations were carried out in the microcanonical ensemble using the velocity Verlet scheme. Periodic boundary conditions, cutoff, etc., were as in the MC simulations. The integration time step was 10 fs. Equilibration and production runs were respectively 500 and 1000 ps. All properties were obtained from positions and velocities stored every 0.1 ps.

The starting configuration for the MC run at 5 K consisted of an $I_h$ (icosahedral) $Ar_{13}$ cluster placed midway between two 12-rings and oriented such that three atoms were along the line joining the centers of two 12-rings. For other temperatures, the starting configuration corresponds to the configuration at the end of equilibration at the previous temperature.

## 4. Results and Discussion

Figure 1 shows a single zeolite L cage with the starting configuration: an icosahedral arrangement of the cluster atoms. Also shown is the configuration at 5 K after equilibration. It is clear that the resulting configuration after equilibration is not icosahedral. In the presence of the field provided by zeolite L, the structure corresponding to the lowest energy configuration for the $Ar_{13}$ cluster is different from the preferred icosahedral geometry of the free cluster.

Table 2 lists the total potential energy of interaction, $\langle U \rangle$, as well as $\langle U_{gg} \rangle$ and $\langle U_{gh} \rangle$ for $Ar_{13}$ in zeolite L between 5 and 33 K. Beyond 33 K, the $Ar_{13}$ cluster splits with one of the atoms separating from the cluster. It is seen that the magnitude of the guest−guest contribution clearly decreases with increase in

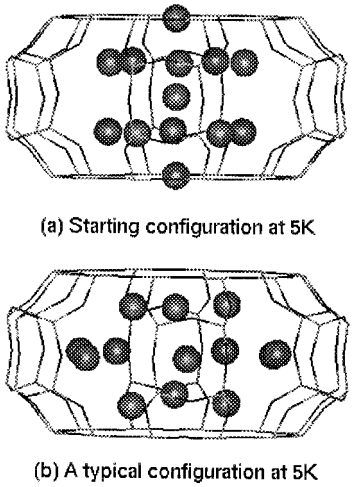


**Figure 1.** (a) Starting configuration: An $I_h$ $Ar_{13}$ in a single zeolite L cage. (b) Typical configuration of the confined $Ar_{13}$ cluster at 5 K.

**TABLE 2: Average Potential Energy of the System as a Function of Temperature**

| $T$ (K) | $\langle U \rangle$ (kJ/mol) | $\langle U_{gg} \rangle$ (kJ/mol) | $\langle U_{gh} \rangle$ (kJ/mol) |
|---|---|---|---|
| 5 | −11.8833 | −2.088 80 | −9.794 51 |
| 8 | −11.8437 | −2.076 39 | −9.767 29 |
| 11 | −11.8040 | −2.068 12 | −9.735 90 |
| 14 | −11.8138 | −2.081 04 | −9.732 74 |
| 17 | −11.7426 | −2.067 68 | −9.674 95 |
| 20 | −11.8552 | −2.041 72 | −9.813 51 |
| 22 | −11.8721 | −2.027 31 | −9.844 83 |
| 24 | −11.8582 | −2.011 90 | −9.846 33 |
| 26 | −11.8315 | −2.006 43 | −9.825 10 |
| 28 | −11.8041 | −1.997 52 | −9.806 57 |
| 30 | −11.7723 | −1.990 34 | −9.781 99 |
| 33 | −11.7289 | −1.981 56 | −9.747 32 |

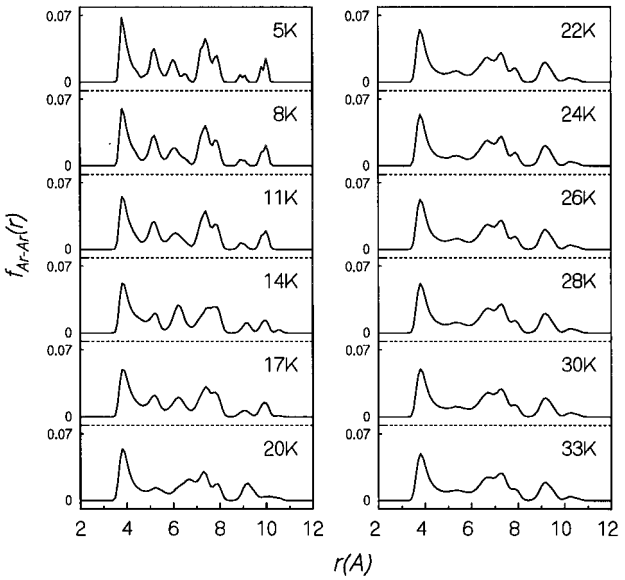


**Figure 2.** Distribution of interparticle distances, $f_{Ar-Ar}(r)$, as a function of temperature.

temperature. This is not necessarily the case with the guest−host contribution. As can be seen from the table, the guest−host contribution is by far the more predominant term. Later, we shall see that it is this term which will play an important role in determining the properties of the cluster.

Figure 2 shows the variation of the distribution of interparticle distances, $f_{Ar-Ar}(r)$ with temperature. The first peak is at about 4 Å, which corresponds to the first peak in the radial distribution function of liquid Ar. It is seen that the distribution changes

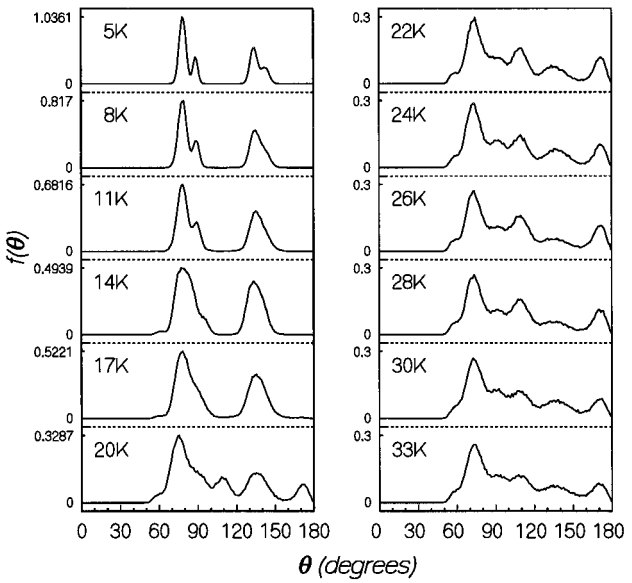


**Figure 3.** Angle distribution function, $f(\theta)$, for different temperatures.

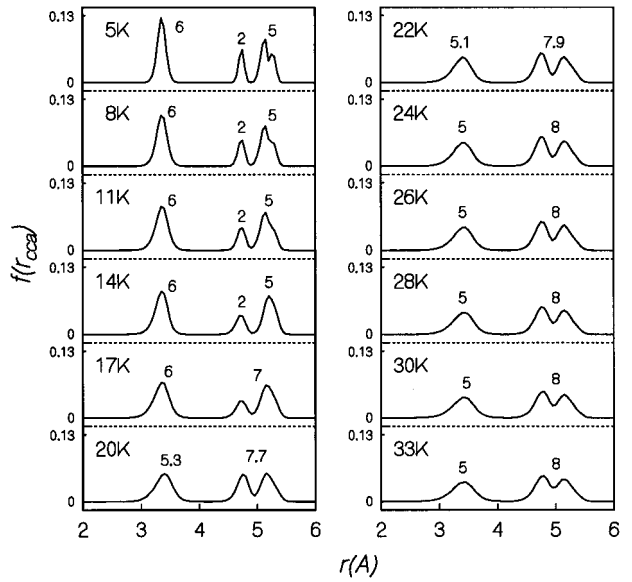


**Figure 4.** Distribution of the distances between a cluster atom and the cage center, $f(r_{cca})$, as a function of temperature.

considerably between 14 and 20 K. Below 14 K, the peaks are sharp while at higher temperatures the peaks are slightly diffuse. The angle distribution function $f(\theta)$ is shown in Figure 3. Here $\theta$ is the angle subtended at the cluster com by any two cluster atoms which lie within a distance of $1.3\sigma$ of the cluster com. Changes in $f(\theta)$ can be seen to occur between 14 and 20 K just as was found in $f_{Ar-Ar}(r)$. $f(\theta)$ at 22 K and above is distinctly more diffuse as compared to the distribution between 5 and 11 K. The nature of $f(\theta)$ and to a certain extent $f_{Ar-Ar}(r)$ suggests changes indicative of rigid to nonrigid transition. As we shall demonstrate below, the present transition differs from the usual solid−liquid transition observed among free clusters in more than one way. Hence, we shall continue to refer to the transition as rigid to nonrigid transition.

The cage center−cluster atom distance distribution function is shown in Figure 4. This gives us an indication about which part of the cage is populated: whether periphery or central region of the cage. Earlier work has suggested that this could play an important role in the diffusion of sorbates.[29,30] Once again, changes in the distribution may be seen between 14 and 20 K, which is reflected by the integrated intensities indicated

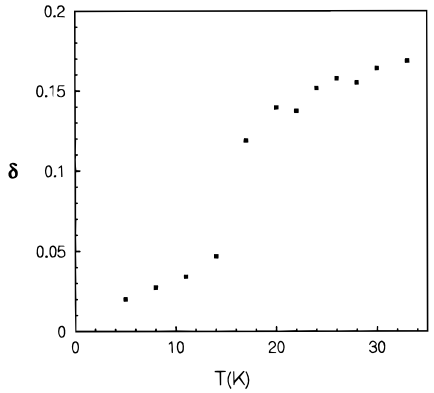


**Figure 5.** Variation of the root-mean-squared pair distance fluctuation, $\delta$, with temperature.

for each peak. At the lowest temperature, 5 K, there are 6, 2 and 5 atoms associated with the three peaks, whereas we have only two peaks at 33 K with intensities 5 and 8.

To understand the nature of this transition between 14 and 20 K that is indicated by the above properties, we looked at several other properties of this cluster. The transition has been often characterized by the use of $\delta$, which is the root-mean-squared pair distance fluctuation given by

$$\delta = \frac{2}{N(N-1)}\sum_{i<j}\frac{(\langle r_{ij}^2\rangle - \langle r_{ij}\rangle^2)^{1/2}}{\langle r_{ij}\rangle} \qquad (6)$$

where $r_{ij}$ are the distances between the guest species and the $\langle\ \rangle$ average implies averaging over the entire run.

This is plotted in Figure 5. There is a significant increase in $\delta$ centered around 17 K, thus confirming the existence of a clear transition in the confined cluster. The value of $\delta$ after the transition is 0.14, which is smaller than the value usually found in free clusters (∼0.25−0.30).[18] However, this value seems to be typical of confined clusters since $Ar_{13}$ in zeolite NaCaA also had a similar value for $\delta$ after the transition.[31] This is, in part, attributed to the fact that the amount of expansion in volume that can be expected for a confined cluster is smaller than that for a free cluster. The volume of the cage in which it is resident provides an upper bound for the volume of the confined cluster. As we shall see later, there are other reasons which contribute to the small value of $\delta$.

Cheng et al.[32] have argued that it is meaningful to define a volume even in the case of a cluster. It would be interesting to see how the volume of the cluster changes with temperature and whether there is a gradual or sharp increase in the volume of the cluster near the transition. There have been some attempts to calculate the volume of the cluster as a function of temperature as well as pressure.[32,33]

We have used the following definition for cluster volume:

$$V_{clus} = \frac{4}{3}\pi\left(r_{av} + \frac{\sigma}{2}\right)^3 = \frac{4}{3}\pi\left[\left(\int_0^\infty r_{cca}\langle f(r_{cca})\rangle\, dr_{cca}\right) + \frac{\sigma}{2}\right]^3 \qquad (7)$$

where $r_{cca}$ is the distance of the argon atom from the cage center. The $\langle\ \rangle$ in $\langle f(r_{cca})\rangle$ indicates that $f(r_{cca})$ is averaged over the whole run as well as over all cluster atoms. Here $r_{av}$ is the average radius of the cluster. Figure 6 gives a plot of the volume of the cluster (as estimated by $r_{av}$) against temperature. The confined cluster clearly shows a sharp change in the volume near the transition. We calculated the variation of $V_{clus}$ with temperature using the radial distribution of atoms from the cluster center of mass in place of $f(r_{cca})$. We did not find any noticeable change from that shown in Figure 6. Cheng et al.[32]

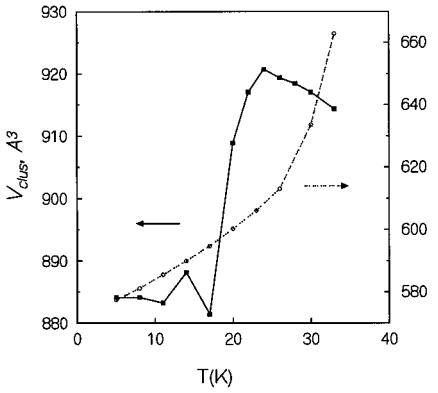


**Figure 6.** Plot of the estimated cluster volume as a function of temperature. The solid line corresponds to the confined cluster and the dotted line to the free $Ar_{13}$ cluster.

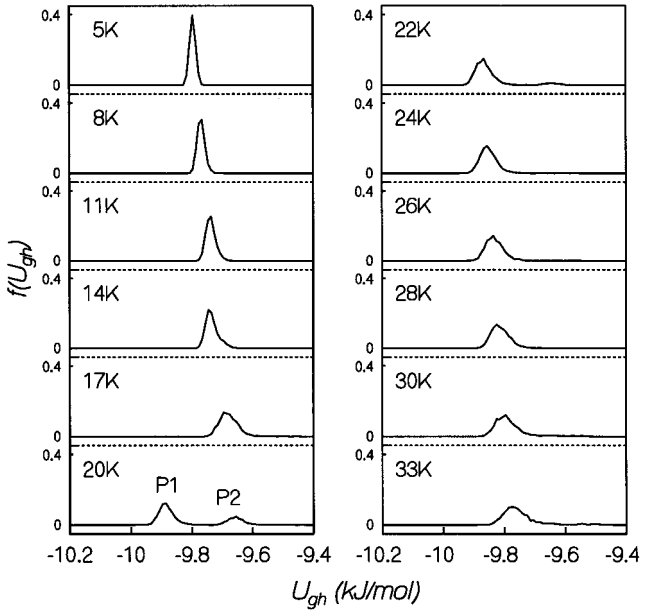


**Figure 7.** Distribution of the short-time averages of $U_{gh}$ at various temperatures. Note that there are two peaks at 20 K.

found a sharp change in the cluster volume near the transition, especially at low pressures, similar to what is shown in Figure 6. However, the results of Cheng et al. are for free $Ar_{55}$ clusters whereas our results relate to $Ar_{13}$ cluster confined in zeolite L. Matsuoka et al.[33] reported that the spatial size of the free $Ar_{79}$ cluster was larger above the transition.

The fact that $\delta$ shows a well-defined transition suggests that there are likely to be two phases as is typically found among free clusters. Figure 7 shows a plot of the distribution of the short-time averages of $U_{gh}$ at various temperatures. At $T = 20$ K, one sees two peaks suggesting coexistence of the two phases. Beyond 20 K, a single peak is observed which is shifted with respect to that found at lower temperatures.

In order to understand better the structure of the two different phases as suggested by the $f(U_{gh})$, we calculated the angle distribution function, $f(\theta)$, separately for peaks P1 and P2. P1 is the peak which has $U_{gh} < -9.73$ kJ/mol, and P2 is the peak that is associated with $U_{gh} > -9.73$ kJ/mol. Figure 8 shows $f(\theta)$ for P1 and P2 calculated separately from configurations corresponding to the two peaks observed at 20 K. Note that the two distributions—though both were obtained at the same temperature—are distinctly different. $f(\theta)$ derived from P1 ($U_{gh}$) $< -9.73$ kJ/mol) configurations resembles closely the $f(\theta)$ at lower temperatures. $f(\theta)$ of P2, on the other hand, is quite similar to the $f(\theta)$ obtained for other temperatures above the

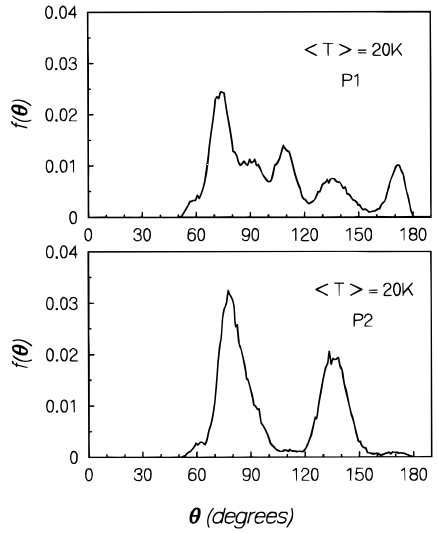


**Figure 8.** Angle distribution function, $f(\theta)$, corresponding to cluster configurations associated with the two peaks in $f(U_{gh})$.

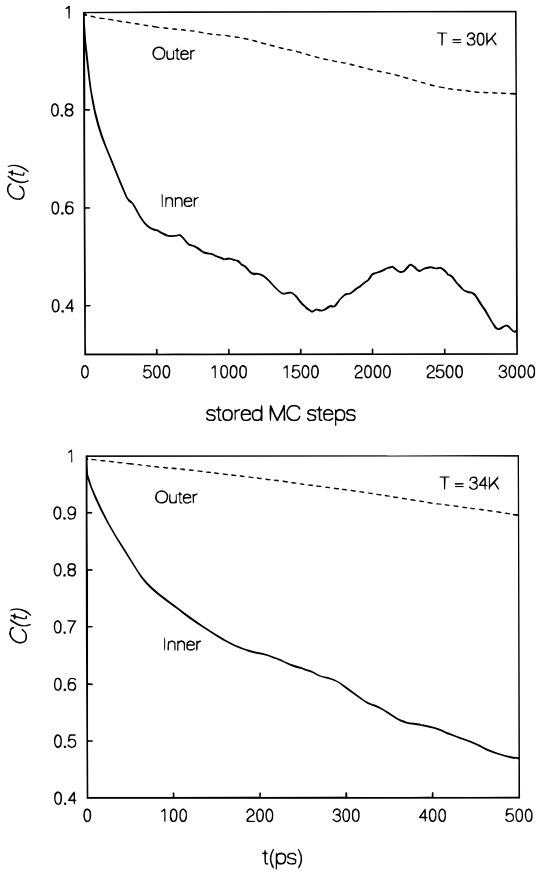


**Figure 9.** Autocorrelation function, $C(t)$, is plotted separately for the inner and outer layers of atoms. The solid line and the dashed line correspond to $C(t)$ for the inner and outer shells of atoms, respectively. (a, top) From MC run at 30 K and (b, bottom) from MD run at 34 K (see text for details).

transition, up to 33 K. This suggests that the phases are distinct both structurally and energetically. Now we shall attempt to look at the dynamical properties associated with the transition.

To obtain a deeper insight into the nature of mobility with which this transition is associated, we performed further analysis of the MC configurations. Earlier work from this laboratory has indicated that the sorbates close to the periphery of the cage and those near the region of the cage center often exhibit considerable differences in their properties.[29,30] The cage itself

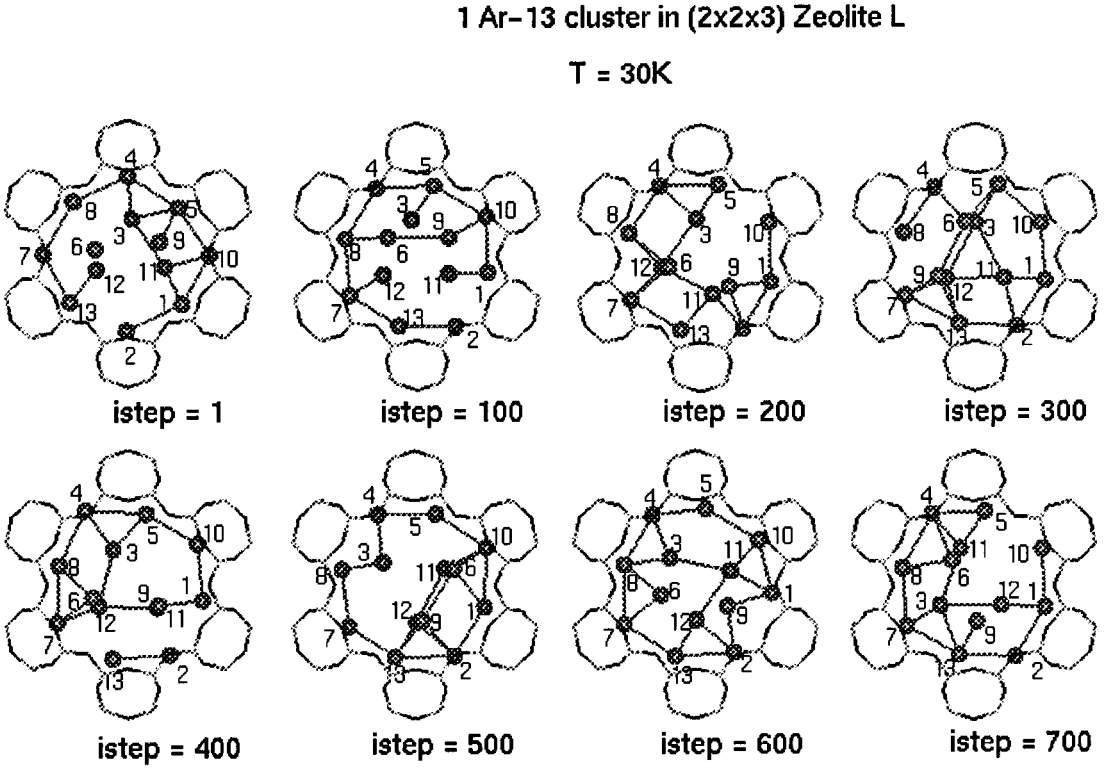


**Figure 10.** Snapshots of $Ar_{13}$ in zeolite L at various MC steps at 30 K. Note that the outer layer of atoms do not rearrange as fast as the inner layer.

has two windows, 12-membered rings or openings. The cage is symmetric about the line joining the centers of the two 12-rings. We define atoms within 3 Å from this axis as inner atoms and those beyond 3 Å as outer atoms. We study the correlation $C(t)$ defined as

$$C(t) = \frac{1}{N(L-t)} \sum_{\tau=0}^{L-t} \sum_{i=1}^{N} \frac{\vec{r}_i(\tau)\cdot\vec{r}_i(\tau+t)}{\vec{r}_i(\tau)\cdot\vec{r}_i(\tau)} \qquad (8)$$

where $\vec{r}_i(\tau)$ is the vector from the cage center to the $i$th cluster atom at $\tau$th MC step. $L$ is the total number of MC steps. $C(t)$ has been calculated separately for the inner (<3 Å) and outer (>3 Å) layers, which is plotted in Figure 9a. Observe that for the inner layer considerable relaxation has ocurred within about 3000 MC steps whereas for the outer layer the correlation function has decayed only to about 0.85 for the same duration. This suggests considerable mobility of the inner layer and little or no mobility of the outer layer. In order to obtain the real time associated with the dynamics of the inner and the outer layers, a new molecular dynamics run was carried out at 34 K for a run length of 3 ns after an equilibration of 3 ns. Figure 9b shows the evolution of $C(t)$. It may be seen that, by about 500 ps, the inner layer atoms have relaxed considerably. In contrast, the outer layers exhibit little relaxation.

Figure 10 shows snapshots of the $Ar_{13}$ cluster in zeolite L at various MC steps at 30 K. The snapshots give further evidence to the observation made in the previous paragraph: the inner atoms rearrange more frequently than the outer atoms. The outer layers seem to remain at the same position for significantly longer durations.

In order to look at the mobility of the $Ar_{13}$ cluster atoms in real time, we carried out microcanonical ensemble molecular dynamics simulations at several temperatures, the details of which have already been given in the previous section. The starting configurations are chosen from the MC runs at the corresponding temperature. The mean-squared displacements

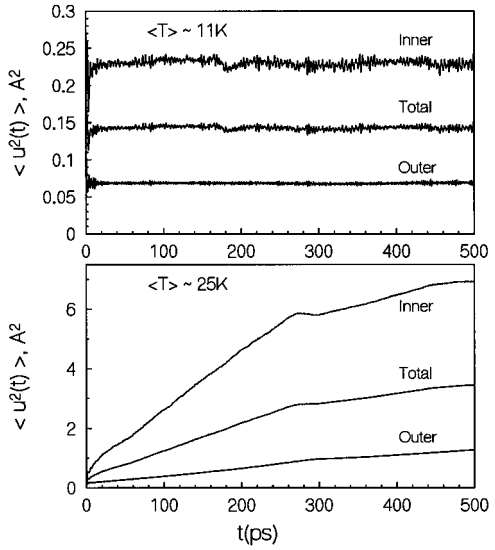


**Figure 11.** Mean-squared displacements for the inner and outer layers of atoms have been plotted as a function of time at 11 and 25 K.

were calculated separately for the inner and outer layers. The result is shown in Figure 11 for a duration of 500 ps at two different temperatures: 11 and 25 K. At 11 K, both inner and outer atoms exhibit little mobility. At 25 K, the inner atoms are significantly more mobile as compared to the outer atoms which are placed in close proximity to the inner wall of the zeolite L cage. It is also seen that by about 300 ps the mean-squared displacement curve for $T = 25$ K levels off. This may be explained as follows. The diameter of an argon atom is 3.4 Å while the cage diameter is 13 Å. Therefore, the available space for inner atoms is $13 - 2(3.4) = 6.2$ Å. However, the finite dimension of the inner atoms permits movement only to the extent $6.2 - 3.4$ Å $= 2.8$ Å whose square is 7.84 Å$^2$, the value around which we should expect $u^2(t)$ to level off. Now, the cage diameter is only approximate since we have chosen to

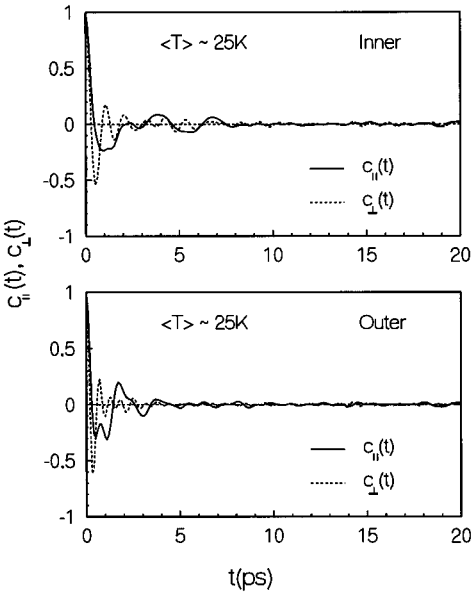


**Figure 12.** Velocity autocorrelation functions, $c_{\parallel}(t)$ and $c_{\perp}(t)$, corresponding to the parallel and perpendicular components of velocity, have been plotted separately for the inner and outer layers at 25 K. Note that the perpendicular components have deeper minima as compared to parallel components. For both parallel and perpendicular components, the minima are deeper for the atoms in the outer layer.

use a highly siliceous zeolite, where Si atoms have been substituted for Ga. Hence, if one takes into account the error involved due to this, the saturation value that is observed is in reasonable agreement with the predicted value.

Earlier we had pointed out that the $\delta$ increases only to 0.14. This may be, in part, due to mobility of only the inner layer atoms. In contrast, in the free $Ar_{13}$ cluster all atoms acquire mobility uniformly. Also, a plot of the mean-squared displacements along the *x*, *y*, and *z* directions indicates that there is virtually no motion along the *z* direction for both inner and outer atoms at 25 K. In other words, the motion of the atoms in the confined cluster seems to be largely two-dimensional, unlike in the free cluster where the atoms can move in three dimensions. This reduction in dimensionality could also lead to a lower value for $\delta$.

In order to characterize the nature of mobility of the inner atoms, we have resolved the velocities of the cluster atoms into parallel and perpendicular components and obtained the respective velocity autocorrelation functions (vafs). The vafs at 25 K are displayed in Figure 12. Here the perpendicular component is defined as

$$\vec{v}_{\perp} = (\vec{v}\cdot\hat{r})\hat{r} \tag{9}$$

where $\hat{r}$ is the unit vector along the line connecting the cage center to the cluster atom. The parallel component is obtained from

$$\vec{v}_{\parallel} = \vec{v} - \vec{v}_{\perp} \tag{10}$$

The power spectra for inner and outer atoms at 11 K as well as at 25 K obtained from the vafs are shown in Figure 13. Some general observations can be made. It is seen that the motion parallel to the cage wall has a vaf with a shallower reflection minimum. In comparison, vafs for motion perpendicular to the wall have deeper minima. This is also true for a single xenon atom sorbed in zeolite−NaY.[34] Also, it is found that the outer atoms always have a larger proportion of high-frequency components (see Figure 13). For both 11 and 25 K, we find that the power spectra associated with the perpendicular

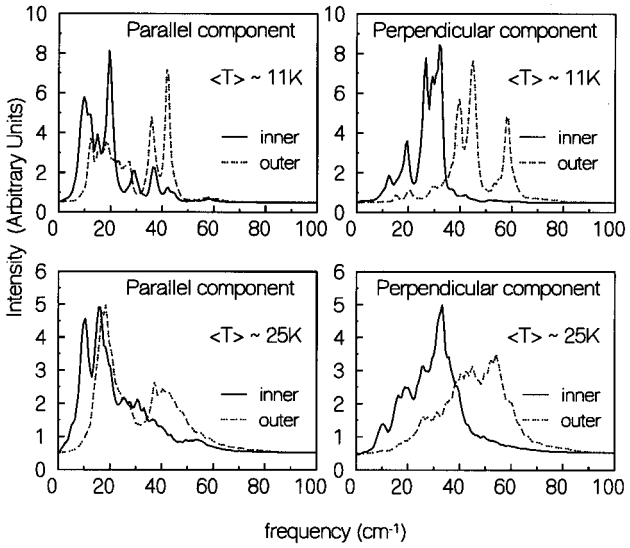


**Figure 13.** Power spectra derived from the velocity autocorrelation functions of the parallel and perpendicular components have been shown at 11 and 25 K. The dotted lines indicate the power spectra for the outer layer and the solid lines for the inner layer of atoms.

component of velocity contain a considerable proportion of high frequencies. In comparison, the power spectra obtained from parallel velocity component have little intensity above ~50 $cm^{-1}$.

The observed behavior which is that the inner atoms acquire mobility even before the outer atoms is surprising. This may be compared with the behavior of free clusters of reasonable size (≥40 atoms) where one can talk of inner and outer atoms. In such clusters, with increase in temperature, the surface atoms (or outer atoms) are far more mobile than atoms in the interior of the cluster. The system can, therefore, be described as a rather rigid solidlike core which is surrounded by a comparatively liquidlike mobile surface. This has been termed "surface melting".[12] In contrast, the $Ar_{13}$ cluster confined in zeolite L seems to consist of a more mobile inner layer surrounded by a relatively slow-moving outer layer of atoms. This opposite trend observed in the confined $Ar_{13}$ cluster can be explained. In the case of free clusters it is the inner atoms which are more strongly bound due to interaction with other cluster atoms. Outer atoms are relatively weakly held, and therefore they "melt" earlier. In the case of confined clusters there is an additional interaction between the argon atoms and the zeolite. This interaction is stronger for the outer layers and rather weak for the inner layer. The argon−zeolite interaction being the predominant interaction, the outer atoms do not acquire mobility whereas the inner atoms do so.

One can conceive of a situation where instead of the small $Ar_{13}$ cluster we have a somewhat larger cluster, say, of 40 or more atoms, confined in a pore (of course, this has to be a mesopore). In such a situation, the interaction of the outer atoms with the zeolite may be comparable with the interaction of the inner atoms with the remaining argon atoms and may lead to a uniform behavior of both the outer and inner atoms, i.e., of the whole cluster. It may be noted that several workers earlier have pointed to the existence of 1/*f* spectra in clusters.[20,22,33] Such spectra have been attributed to the existence of different relaxation times in the system. Assuming that the same argument is valid for confined clusters, similar 1/*f* behavior may be expected. Now consider a cluster which is confined in a host matrix where the interactions with the host are comparable to the interactions among the atoms of the cluster. Under this condition, the surface atoms lose their surface characteristics,

effectively, giving rise to a cluster without a surface! For such a cluster of atoms, one would expect an absence of a whole spectrum of relaxation times and consequently no $1/f$ spectra. It would be interesting to try and design such a system and see whether indeed this is true. Experimentally, the system that would probably come closest to this specification may be a cluster of carbon atoms enclosed, for example, in a carbon nanopore.

## 5. Conclusions

The main conclusions of the study of $Ar_{13}$ cluster confined in zeolite L are the following:

The icosahedral geometry is no longer the preferred arrangement of the cluster atoms in the presence of the field provided by zeolite L. The confined cluster shows a well-defined transition indicated by the $\delta$ vs $T$ plot, which exhibits an abrupt rise between 14 and 20 K. This may be compared to the free cluster which melts around 27 K. Coexistence is observed during the transition.

Unlike in free clusters of size greater than 40 where the outer shell of atoms acquire mobility before the inner core, in the confined cluster the mobility of inner shell of atoms precedes that of outer shell of atoms. The inner shell of atoms exhibit larger mobility than the outer shell of atoms, this in spite of the fact that the inner shell has lesser volume in which to move about. However, the inner shell of atoms soon reaches the maximum possible displacement. The opposite trend in the case of a confined cluster as compared to medium to large free clusters is attributed to the strong interaction between the outer layer atoms and the atoms of zeolite L. One expects that under certain conditions when the outer atom interaction with the host and the inner atom interaction with the remaining cluster atoms would be comparable, the cluster would not possess multiple relaxation times and consequently will not exhibit $1/f$ spectra.

**Acknowledgment.** The authors acknowledge the excellent computational facilities provided by the Supercomputer Education and Research Centre, Indian Institute of Science, for carrying out this work. The authors thank the referee for bringing the work of Cheng et al. to their attention. The authors also thank the Department of Science and Technology, Government of India, for partial support of this research.

## References and Notes

(1) Berry, R. S.; Cheng, H.-P. *Physics and Chemistry of Finite Systems: From Clusters to Crystals*; Kluwer Academic Publishers: Dordrecht, 1992; Vol. I, p 277.
(2) Beck, T. L.; Marchioro II, T. L. *Phys. Rev. A* **1990**, *42*, 5019.
(3) Hoare, M. R.; Pal, P. *Nature* **1970**, *230*, 5.
(4) McGinty, D. J. *J. Chem. Phys.* **1973**, *58*, 4733.
(5) Briant, C. L.; Burton, J. J. *J. Chem. Phys.* **1975**, *63*, 2045.
(6) Etters, R. D.; Kaelberer, J. *Chem. Phys.* **1977**, *66*, 5112.
(7) Etters, R. D.; Kaelberer, Phys. *Rev. A* **1975**, *11*, 1068.
(8) Honeycutt, J. D.; Andersen, H. C. *J. Phys. Chem.* **1987**, *91*, 4950.
(9) Adams, J. E.; Stratt, R. M. *J. Chem. Phys.* **1990**, *93*, 1332.
(10) Quirke, N.; Sheng, P. *Chem. Phys. Lett.* **1984**, *110*, 63.
(11) Frantz, D. D. *J. Chem. Phys.* **1995**, *102*, 3747.
(12) Nauchitel, V. V.; Pertsin, A. J. *Mol. Phys.* **1980**, *40*, 1341.
(13) Li, F.-Y.; Berry, R. S. *J. Phys. Chem.* **1995**, *99*, 2459.
(14) Li, F.-Y.; Berry, R. S. *J. Phys. Chem.* **1995**, *99*, 15557.
(15) Berry, R. S. *Z. Phys. D* **1989**, *12*, 161.
(16) Berry, R. S. *J. Chem. Soc., Faraday Trans.* **1990**, *86* (13), 2343.
(17) Jellinek, J.; Beck, T. L.; Berry, R. S. *J. Chem. Phys.* **1986**, *84*, 2783.
(18) Beck, T. L.; Jellinek, J.; Berry, R. S. *J. Chem. Phys.* **1987**, *87*, 545.
(19) Davis, H. L.; Jellinek, J.; Berry, R. S. *J. Chem. Phys.* **1987**, *86*, 6456.
(20) Nayak, S. K.; Ramaswamy, R. *Proc. Indian Acad. Sci., Chem. Sci.* **1994**, *106*, 521.
(21) Nayak, S. K.; Ramaswamy, R. *J. Phys. Chem.* **1994**, *98*, 9260.
(22) Nayak, S. K.; Ramaswamy, R. *Phys. Rev. Lett.* **1995**, *74*, 4181.
(23) Berry, R. S. *Chem. Rev.* **1993**, *93*, 2379.
(24) Berry, R. S. *Int. J. Mod. Phys. B* **1992**, *6*, 3695.
(25) Berry, R. S. *J. Phys. Chem.* **1994**, *98*, 6910.
(26) Wright, P. A.; Thomas, J. M.; Cheetham, A. K.; Nowak, A. K. *Nature* **1985**, *318*, 611.
(27) Henson, N. J.; Cheetham, A. K.; Peterson, B. K.; Pickett, S. D.; Thomas, J. M. *J. Comput.-Aided Mater. Des.* **1993**, *1*, 41.
(28) Allen, M. P.; Tildesley, D. J. *Computer Simulation of Liquids*; Clarendon Press: Oxford, 1987.
(29) Yashonath, S.; Santikary, P. *J. Phys. Chem.* **1993**, *97*, 3849.
(30) Yashonath, S.; Santikary, P. *J. Phys. Chem.* **1993**, *97*, 13778.
(31) Chitra, R.; Yashonath, S. Submitted for publication.
(32) Cheng, H.-P.; Li, X.; Whetten, R. L.; Berry, R. S. *Phys. Rev. A* **1992**, *46*, 791.
(33) Matsuoka, H.; Hirokawa, T.; Matsui, M.; Doyama, M. *Phys. Rev. Lett.* **1992**, *69*, 297.
(34) Yashonath, S. *Chem. Phys. Lett.* **1991**, *177*, 54.
(35) Kunz, R. E.; Berry, R. S. *Phys. Rev. Lett.* **1993**, *71*, 3987.
(36) Sasai, M.; Ohmine, I.; Ramaswamy, R. *J. Chem. Phys.* **1992**, *96*, 3045.